Dilute Solution Properties of Poly[N-(n-octadecyl)maleimide]. 3. Realistic Hydrodynamic Calculation of Intrinsic Viscosity for This Comblike Structure

Juan J. Freire

Departamento de Química Física, Facultad de Ciencias Químicas, Universidad Complutense, Madrid 3, Spain

José M. Barrales-Rienda and Carmen Romero Galicia

Instituto de Plásticos y Caucho, CSIC, Madrid 6, Spain

Arturo Horta*

Departamento de Quimica General y Macromoléculas, Facultad de Ciencias, Universidad a Distancia (UNED), Madrid 3, Spain. *Received April 15, 1982*

ABSTRACT: The intrinsic viscosity of poly[N-(n-octadecyl)maleimide] (PMI-18) is calculated by means of a realistic model that takes into account the hydrodynamics of the different chain elements. The theoretical results obtained in this way give a good description of experimental data obtained in previous work. An equivalent wormlike chain allows us to describe the data in the range of high molecular weights, where the detailed model cannot be applied. For the low molecular weight range, however, the wormlike chain is shown to be inadequate. The influence of interactions between neighboring side chains on the hydrodynamic properties of the chain is qualitatively analyzed.

Introduction

The intrinsic viscosity measured on poly[N-(n-octadecyl)maleimide] fractions over a wide range of molecular weights from the oligomers up to high M's ($10^3 < M_n < 200 \times 10^3$) has shown a complex $[\eta]$–M dependence, in which the simple Mark–Houwink equation with constant parameters K and a is not followed.[1] This polymer has a comblike structure with long, flexible alkyl side chains attached to a semistiff backbone composed of maleamic rings. The theoretical calculation of the intrinsic viscosity of this complex molecular structure and the comparison of results with the experimental data previously reported[1] are the object of this paper.

To explain on a quantitative basis the observed deviations from the simple Mark–Houwink law and the extremely small values found for the exponent a ($0 \lesssim a \lesssim 0.2$) in the low molecular weight region ($M_n \lesssim 12 \times 10^3$), the theoretical calculations should consider the contribution of the following facts: (1) The special arrangement of the chemical groups in a comblike structure gives an averaged form to the chain very different from that expected for a linear polymer. (2) The data cover a region of low molecular weights, where a detailed hydrodynamic description of the different chain elements ought to be considered. (This effect can also be observed in linear chains, especially in those with a wide cross section.[2]) (3) There are complicated interactions between the solvent molecules and the polymer chemical groups. These interactions create correlations between polymer groups belonging to neighboring branches (long-range interactions). Though polymer–solvent interactions also play an important role in the backbone excluded volume effects of high molecular weight polymers, their influence on the configuration of side chains is mainly manifested together with factors 1 and 2 in the study of the shortest chains, for which local shape effects have a noticeable contribution to the global hydrodynamic behavior of the polymer.

In order to explain the experimental data, we have divided the total range of molecular weights into two regions. The first includes chains with up to 100 repeating units ($n \lesssim 100$). In this region we apply a theoretical realistic hydrodynamic formalism that takes into account the first two factors described above. The polymer–solvent interactions cannot be conveniently tackled by any current theory. They will be, however, qualitatively studied in the final comparison of the theoretical results with the experimental data.

In the second region, which covers longer chains characterized by $n > 100$, the realistic hydrodynamic formalism cannot be applied, as it involves extremely tedious numerical calculations. Fortunately, it is possible to neglect most details of the chemical structure in this region so that, when excluded volume effects are ignored, the experimental data can be accounted for with a simple parametric model of rigidity such as the well-known wormlike chain.

Hydrodynamic Theory for Short Chains

Our calculations for short chains are based on a general expression for the intrinsic viscosity of a polymer chain in solution derived from the Kirkwood–Riseman theory with preaveraged Oseen treatment of the hydrodynamic interactions between polymer segments.[3,4] This expression can be written as

$$[\eta] = (N_A/6M\eta_0)\sum_{i=1}^{N_T}\sum_{j=1}^{N_T} f_j(\mathbf{H}^{-1})_{ij}\langle \mathbf{R}_i \cdot \mathbf{R}_j \rangle \qquad (1)$$

where N_A is Avogadro's number, M is the polymer molecular weight, N_T is the total number of theoretical hydrodynamic units included in the model, η_0 is the solvent viscosity, and f_j if the friction coefficient of the jth unit. $\mathbf{H}$ is the hydrodynamic interaction matrix, whose elements are[5]

$$H_{ij} = 1, \qquad i = j \qquad (2)$$

$$H_{ij} = (f_i/6\pi\eta_0)\langle R_{ij}^{-1} \rangle, \qquad i \neq j$$

where $\langle R_{ij}^{-1} \rangle$ is the averaged reciprocal distance between units i and j.

Equation 1 includes other geometrical averages $\langle \mathbf{R}_i \cdot \mathbf{R}_j \rangle$ that represent the equilibrium correlation functions corresponding to the positions of units i and j with respect to the center of masses of the chain. These averages are easily evaluated in terms of the mean quadratic distances between units, $\langle R_{ij}^2 \rangle$, through the relations[5]

$$\langle \mathbf{R}_i \cdot \mathbf{R}_j \rangle = \tfrac{1}{2}[\langle R_i^2 \rangle + \langle R_j^2 \rangle - \langle R_{ij}^2 \rangle] \qquad (3)$$

$$\langle R_i^2 \rangle = N_T^{-1}\sum_{i=1}^{N_T} \langle R_{ij}^2 \rangle - \langle S^2 \rangle \qquad (4)$$

0024-9297/83/2216-0946$01.50/0

$$\langle S^2 \rangle = N_T^{-2} \sum_{i>j}^{N_T N_T} \sum \langle R_{ij}^2 \rangle \quad (5)$$

where $\langle S^2 \rangle$ is the mean-square radius of gyration of the chain. Therefore, the calculation of the intrinsic viscosity implies an evaluation of all the different mean quadratic and reciprocal distances between groups.

More rigorously, the positions should be referred to the chain's hydrodynamic center,[6] which complicates the computation of the correlations. In fact, we have also considered an equivalent expression given by Fixman and Kovac[7]

$$[\eta] = (N_A/6M\eta_0) \sum_{i}^{N_T N_T} \sum_{j} f_j \langle \mathbf{b}_i \cdot \mathbf{b}_j \rangle (\mathbf{B}^{-1})_{ij} \quad (6)$$

where $\langle \mathbf{b}_i \cdot \mathbf{b}_j \rangle$ represents the correlation between the bond vectors $\mathbf{b}_i$ and $\mathbf{b}_j$ (i.e., the bonds joining units $i-1$ to i and $j-1$ to j). The evaluation of these correlations will be described later. $\mathbf{B}$ is a matrix defined as

$$\mathbf{B}_{ij} = H_{ij} - H_{i,j-1} - H_{i-1,j} + H_{i-1,j-i}; \qquad i = 1, ..., N_T - 1 \quad (7)$$

Since eq 6 depends only on the relative positions between units, it should give the same values for $[\eta]$ as the rigorous version of eq 1.[8] Nevertheless, the form of eq 1 will be needed to introduce further approximations. We have obtained some results with the simplified version of eq 1 (i.e. referring positions to the center of masses) and with eq 6, and we have verified that both kinds of numerical values agree within a 1% error range. In consequence, the reference to the center of masses is a quite good approximation for our purposes.

In order to obtain the averaged distances $\langle R_{ij}^{-1} \rangle$ and $\langle R_{ij}^2 \rangle$ we should consider a detailed statistical model for the polymer chain. In this work we are guided by the rotational isomeric model,[9] which considers realistic bond lengths, bond angles, and energetic short-range interactions describing the internal rotations of the groups. However, we have introduced several approximations that somewhat simplify the calculations for the comblike chains studied here: (1) We consider, in principle, that the main chain is in a rigid "threo-disyndiotactic" configuration, since it is apparent that this configuration is predominant for structures of this kind.[10] Then, using crystallographic data for the atomic distribution in the maleimide molecule[11] and taking *n*-alkane bond lengths and angles for the C–C–C joints between maleamic rings, we have estimated that the distance between successive nitrogen atoms is about 5.73 Å, adopting an "all-trans" configuration along the main chain with "virtual bond" angles of 48.8°. Deviations from the fully rigid main chain described in this way will be introduced later by means of a flexibility parameter. (2) We assume a free rotation for the first C–C bond of every side chain with respect to the C–N bond that joins it to the main chain. This approximation (in part justified by the symmetry of the interactions corresponding to the first groups in the side chains with respect to the closest heterocycle in the main chain) has the advantage of avoiding a complex study of the conformational energies associated with the rotation, which would yield only a modest improvement in the accuracy of the final results. (3) In order to reduce the number of hydrodynamic units included in the chain scheme, different chemical groups of every repeating unit are embedded in spherical "hydrodynamic beads", which are designed to represent, in a first approximation, the hydrodynamic behavior of these groups considered as a whole. Thus, as shown in Figure 1, we join every two successive nitrogen atoms along the main chain

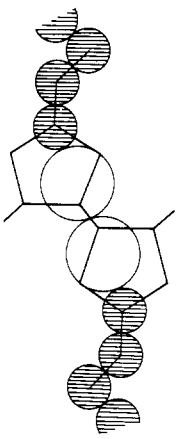

Figure 1. Hydrodynamic units in a threo-disyndiotactic configuration (dyad).

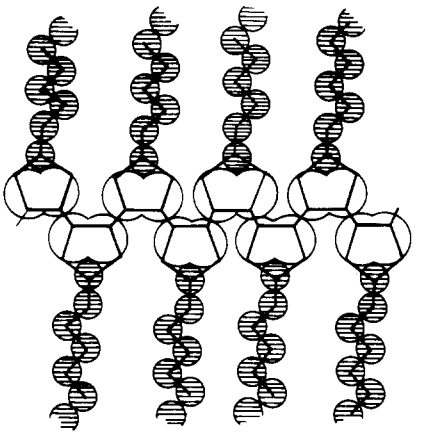

Figure 2. Hydrodynamic units in threo-disyndiotactic configuration (sequence).

by means of an array of four spheres in contact. Two of them (beads A) have the diameter of a C–C bond (d_A = 1.53 Å) while the other two between them (beads B) are bigger (d_B = 2.10 Å). Beads A are also used to represent the methylene groups, CH_2, along the *n*-alkyl side chains.

The global chain scheme in terms of the "hydrodynamical beads" is shown in Figure 2, where we can notice some overlapping between neighboring units B attached to the same unit A. Though a realistic Oseen tensor treatment would not be rigorously correct for overlapping spheres, the simplest Oseen tensor version given in eq 1 and 2 considers point beads so that their size is taken into account only through the Stokes law formula, which establishes a direct proportionality between friction coefficients and diameters. (It should be noted that the use of the Stokes law eliminates the dependence of the calculations on the solvent viscosity.) Moreover, the overlapping is extended only to a very reduced fraction of the total hydrodynamic volume of the chain.

The evaluation of the averages $\langle R_{ij}^2 \rangle$ for our model is performed by applying the recursion relation[9]

$$\langle R_{ij}^2 \rangle = -2\langle \mathbf{b}_i \cdot \mathbf{b}_j \rangle - \langle R_{ia,ja}^2 \rangle + \langle R_{i,ja}^2 \rangle + \langle R_{ia,j}^2 \rangle \quad (8)$$

with

$$\langle R_{1k}^2 \rangle = 2 \sum_{k'}^{ka} \langle \mathbf{b}_{k'} \cdot \mathbf{b}_k \rangle + \langle \mathbf{b}_k \cdot \mathbf{b}_k \rangle + \langle R_{1,ka}^2 \rangle \quad (9)$$

where ka corresponds to the unit preceding bead k (i.e., the main-chain bead attached to bead k, if k is the first unit of a side chain, and the bead $k-1$ otherwise). Index k' in eq 9 runs over all the units placed along the shortest path of bonds going from bead 1 to bead ka.

For beads belonging to the rigid backbone, the evaluation of $\langle \mathbf{b}_i \cdot \mathbf{b}_j \rangle$ is trivial. It is also straightforward to obtain these averages for beads belonging to the same side chain. In fact, we take two different representations for the *n*-alkyl side chains. In the first, they are assumed to be "all-trans" *n*-alkane conformations, with a bond angle of 112°. It should be remarked that this representation does not correspond to a completely rigid polymer molecule, since we have introduced some flexibility by considering free rotation for every side chain's first C–C bond.

In the second representation side chains are substituted by realistic *n*-alkane chains for which we know the averages $\langle R_{ij}^2 \rangle$ and $\langle R_{ij}^{-1} \rangle$ from previous Monte Carlo calculations.[12] Then the $\langle \mathbf{b}_i \cdot \mathbf{b}_j \rangle$ are obtained with this model by application of eq 8 to these simple linear chains.

The assumption of free rotation for the side chain's first bond simplifies the computation of the rest of the $\langle \mathbf{b}_i \cdot \mathbf{b}_j \rangle$. Thus the correlations between any side-chain bond vector and the one corresponding to the C–N bond joining the side chain to the backbone (C–N joints) have a non-null component only in the direction of the latter bond. This direction is, on the other hand, well defined with respect to those of the backbone's bond vectors and also with respect to those of the other C–N joints, which allows us to obtain easily all the different $\langle \mathbf{b}_i \cdot \mathbf{b}_j \rangle$.

Once all the different bond correlations have been calculated, we introduce a correction to take into account the possible flexibility of the main chain. Thus we consider a parameter α whose numerical value must be slightly smaller than one so that $1 - \alpha$ describes the loss of correlation between bond vectors due to the deviation from total rigidity of the joints between successive repeating units. The parameter α is easily related to those used to describe flexibility in simpler stiff polymer models such as the persistence length in the wormlike chain.[5] Then if beads i and j belong to different repeating units m_i and m_j, the correction for flexibility is expressed by

$$\langle \mathbf{b}_i \cdot \mathbf{b}_j \rangle = \langle \mathbf{b}_i \cdot \mathbf{b}_j \rangle_{\text{rigid}} \alpha^{|m_i - m_j|} \tag{10}$$

and these corrected correlations are placed in eq 8 and 9 in order to obtain the mean quadratic distances.

We also need the mean reciprocal averages $\langle R_{ij}^{-1} \rangle$. These quantities could be obtained exactly for our model only through time-consuming simulation techniques. However, we can easily make a fair estimation of their value. For rigid parts of the chain $\langle R_{ij}^{-1} \rangle = \langle R_{ij}^2 \rangle^{-1/2}$. Moreover, we have previously calculated[12] both the mean reciprocal and quadratic distances for realistic *n*-alkane chains, which constitute our nonrigid representation of the side chains. Consequently, if we consider now two beads i and j placed in two different subchains, the shortest path of bonds between them can be divided into two or three regions, with different statistics (flexible or rigid). Defining

$$f_{ij}^{-2} = \sum_{k=1}^{n_r} \langle R_{lm}^2 \rangle / \sum_{k=1}^{n_r} [\langle R_{lm}^{-1} \rangle]^{-2} \tag{11}$$

where l and m correspond to the terminal beads of every one of the n_r regions considered along the path, f_{ij} enables us to estimate $\langle R_{ij}^{-1} \rangle$ as

$$\langle R_{ij}^{-1} \rangle = f_{ij} \langle R_{ij}^2 \rangle^{-1/2} \tag{12}$$

Since the values of f_{ij} range from 1 (for a rigid chain) to 1.09 (for a realistic nonadecane chain),[12] the estimation of $\langle R_{ij}^{-1} \rangle$ seems to be accurate enough and should not introduce significant errors in the final results for $[\eta]$ ($f_{ij} = 1$ would be also a good approximation for these semistiff structures).

The practical use of eq 1 or 6 to the calculation of theoretical results for the intrinsic viscosity is limited by the high number of hydrodynamic units involved in the model (21 for every repeating unit). From the computational point of view, the most critical step of the procedure is the inversion of matrix **H**, which requires its previous storage. In order to avoid this problem, we have obtained our results by means of an approximate version of eq 1 that can be written as

$$[\eta] = (N_A/6M\eta_0)[\sum_{i=1}^{N_T} f_i \langle R_i^2 \rangle] \times [1 + (\sum_{i=1}^{N_T} f_i \langle R_i^2 \rangle)^{-1} \sum_{i \neq j}^{N_T N_T} \sum f_j H_{ij} \langle \mathbf{R}_i \cdot \mathbf{R}_j \rangle]^{-1} \tag{13}$$

Equation 13 as an approximate substitute of eq 1 for $[\eta]$ can be considered to be equivalent to the well-known 1953 Kirkwood equation for the translational diffusion coefficient, D_t, in terms of the elements H_{ij}, which is often utilized instead of the more rigorous (and $\mathbf{H}^{-1}$ dependent) 1948 Kirkwood formula[4,13]. In fact, eq 13 can be obtained as the orientationally and configurationally preaveraged version of the expression for the intrinsic viscosity derived by Tsuda.[14] In Table I we show the results obtained with eq 1 and 13 for completely rigid-backbone chains ($\alpha = 1$). From these results (calculated for the shortest samples of the comblike structures with the realistic *n*-alkane representation for side chains), it can be observed that differences between the values given by eq 1 and 13 increase slowly with increasing number of repeating units. Furthermore, the errors of the approximate formula tend to a constant value for the highest values of N. From previous similar calculations for different types of chain,[15] we have learned that the errors soon reach a constant value or a maximum, which we estimate in this case to be around 15%. Then eq 13, though less accurate than the approximate Kirkwood formula for D_t, gives estimated errors comparable to those of most experimental results and, in consequence, can be applied to the calculations for longer chains.

Table I
Theoretical Intrinsic Viscosities from Eq 1 and 13 for Completely Rigid Main Chains ($\alpha = 1$) and Flexible Side Chains

	$[\eta]$, cm^3 g^{-1}	
n	eq 1	eq 13
2	3.36	3.14
3	2.87	2.64
4	2.75	2.47
5	2.64	2.35
6	2.62	2.31

The elements H_{ij} and the averages $\langle \mathbf{R}_i \cdot \mathbf{R}_j \rangle$ involved in eq 13 can be simply calculated at the time their indices are run in the double sum. It is desirable, however, to store the averages $\langle R_{ij}^{-1} \rangle$ and $\langle R_{ij}^2 \rangle$ since their calculation includes additional sums. Fortunately, the storage does not require a number of numerical elements proportional to $N_T \times N_T$, for the structure of the chain allows us to use some symmetry properties. Thus all couples of beads placed in equivalent positions along side chains separated by the same number of repeating units have the same distance averages. In consequence, the averages can be calculated and stored for $n \ll 100$ employing a reasonable amount of computer time and memory positions.

Wormlike Chain Calculations

For chains with more than 100 repeating units, the realistic treatment based on hydrodynamic beads cannot be afforded, due to numerical limitations. For these longer chains, whose estimated cross section is at least 5 times

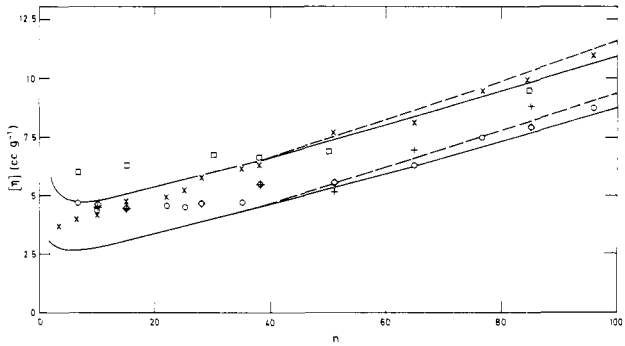

Figure 3. Intrinsic viscosities for chains of varying lengths. The lower and upper curves describe the theoretical results obtained for the realistic model with the flexible and "all-trans" side-chain representations, respectively: solid lines, $\alpha = 0.94$ ($l = 79$ Å); broken lines, $\alpha = 0.95$ ($l = 95$ Å). Experimental data in tetrahydrofuran (×), *o*-dichlorobenzene (□), toluene (◇), α-chloronaphthalene (+), and benzene (○) are also included.

smaller than their longitudinal length, the use of wormlike chains seems adequate. A wormlike chain consists of an infinite number of very small hydrodynamic units joined so that the correlation between two succesive units is given by[5] $\cos\theta = -\alpha$. The model includes several parameters. One of them, L, describes the chain's contour length (proportional to its molecular weight). A second parameter, called the persistence length, $l/2$, describes the stiffness. Its relation with our flexibility parameter is[5]

$$l/2 = b/(1 - \alpha) \tag{14}$$

where b is the length of the repeating unit. In our case, b can be conveniently obtained as half the distance between every two second-neighbor nitrogen atoms along the main chain ($b = 2.38$ Å). Moreover, the model contains a third parameter, d, accounting for the cross section of the chain.[16] For the shortest chains, the model reduces to a spheroid cylinder.[17] The shape of the hemispheroids placed at the ends of the cylinder is characterized by means of the parameter ϵ. Over the past several years, a new parameter has been incorporated into the model in order to take into account correlations between the curvatures of the chain. The resulting model is called the helical wormlike chain.[18] We will not consider here the latter parameter since our discrete model does not include correlations of this kind and, on the other hand, the experimental results do not exhibit oscillations that would reveal the presence of significant helix participation. It will be shown in next section that the results are fairly predicted by a simple wormlike chain in the region of high molecular weights, where the helical contribution could be relevant.

In order to obtain results for $[\eta]$ with the wormlike chain, we have employed the formulas derived by Yamakawa and Fujii[16] in the revised and generalized version given by Yamakawa and Yoshizaki.[17] That is, we have performed our calculations with eq 37 and 38 of ref 16 together with eq 23–33 of ref 17 (eq 30 of ref 17 contains a typographical error that is easily corrected by comparing the expression with eq 108 of ref 19).

Results and Discussion

From eq 2–5 and 8–13 we have obtained theoretical results for the intrinsic viscosity of our discrete model in the region $n \leq 100$ with different values of α and considering the rigid "all-trans" and the realistic (flexible) *n*-alkanes as representations for the side chains. The results for $\alpha = 0.94$ and $\alpha = 0.95$ are summarized in Figure 3, where they are compared with experimental data obtained in different solvents. The curvature of the experimental

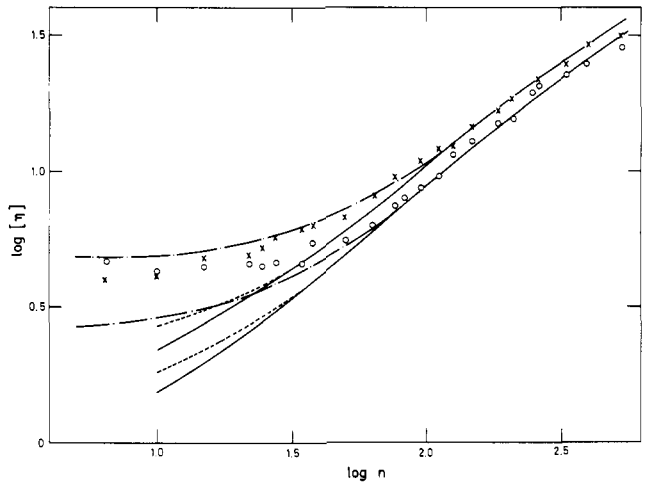

Figure 4. Logarithmic representation of intrinsic viscosities of chains of varying lengths. The dot–dash lines describe the theoretical results for the realistic model with flexible (lower curve) and "all-trans" (upper curve) side chains. The continuous lines describe the results for the wormlike chain with $\epsilon = 1$ and $d/l = 0.20$ (lower curve) and $d/l = 0.26$ (upper curve). The broken lines describe the low molecular weight results of the same wormlike chains with $\epsilon = 0.6$. In all cases the value $\alpha = 0.94$ ($l = 79$ Å) is adopted. Experimental data in tetrahydrofuran (×) and benzene (○) are also included.

data for the highest molecular weights in this region is adequately described with the value $\alpha = 0.94$. It can be observed that the results of the rigid side chain representation for this value of α agree closely with the data corresponding to tetrahydrofuran except for the lowest molecular weights. The same representation is also fairly consistent with the data obtained in *o*-dichlorobenzene. However, the flexible side chain representation gives results closer to the experimental intrinsic viscosities in benzene and toluene, while the α-chloronaphthalene set of data presents an intermediate behavior between both representations.

The value $\alpha = 0.94$ for the flexibility parameter corresponds through eq 14 to a wormlike chain with the value $l = 79$ Å for the statistical segment length. In Figure 4 we have plotted the results for equivalent wormlike chains with cross sections $d/l = 0.20$ and 0.26 and $\epsilon = 1$ (prolate spheroid cylinder limit). The results for $d/l = 0.26$ are obtained under the assumption that the formulas for $L/l > 2.278$ and $d/l \leq 0.2$ in ref 17 are sufficiently accurate even in this case. In Figure 4 we have drawn the experimental data in tetrahydrofuran and benzene for the whole range of molecular weights and they seem to agree with the wormlike chain curves for high n's. This agreement is facilitated because we have taken for α the value already determined with the discrete model for the low-n region. It should also be considered that we have at hand a range of molecular weights wide enough for an easy fitting of the model to the experimental data. We can observe in Figure 4 that the theoretical results for the discrete model and the wormlike chain become coincident for the highest values of n included in the calculations of the low molecular weight range ($n \leq 100$). This implies that for $n > 100$ the wormlike chain seems adequate to reproduce the actual hydrodynamic behavior of this type of comblike polymers. The value of the statistical segment length serves as an estimation of the flexibility inherent to the main chain with respect to the rigid "threo-disyndiotatic" configuration. However, the actual value determined for l may contain the influence of the backbone excluded volume (as we discussed previously[1]), since this effect is not dealt with separately in the model. But we expect this effect of

backbone excluded volume to be small, because with l = 79 Å, the number of statistical segments in the PMI-18 chains is low (less than 20), even for the highest molecular weight fractions.

Figure 4 also shows that for small values of n ($n < 90$), the wormlike model cannot account for the absolute values and trends of the experimental data. Changes in the parameter ϵ (which defines the form of the spheroid cylinder in the short-chain limit) do not improve significantly the agreement between the wormlike results and the data. In Figure 4 we have included the results calculated with ϵ = 0.6, the lower limit of ϵ for which the analytical formulas of ref 17 are valid. These results are slightly closer to the experimental values than those corresponding to $\epsilon = 1$ but, nevertheless, they lie fairly far away from the data. Moreover, since the shortest comblike polymers have a hydrodynamic shape very different from those of simple geometrical bodies, we believe that their transport properties can only be described by means of detailed models similar to the discrete chain outlined in this work.

Figure 4 reveals that the rigid-chain representation is closer to the general experimental behavior than the flexible one for the lowest molecular weights, though the latter representation better describes the data obtained in benzene for longer chains. In fact, most of the experimental data corresponding to the different solvents lie between our two theoretical curves, as Figure 3 shows clearly. However, differences between the several sets of data are noticeable. We believe that these differences are caused by the influence of interactions between solvent molecules and polymer segments on the long-range intramolecular interactions between polymer groups belonging to neighboring side chains. The steric effects tend to align these chains in a direction perpendicular to the backbone's longitudinal axis. Then the side chains should be less flexible than the corresponding isolated n-alkanes. The solvent-dependent alignments play an important role in the global hydrodynamic behavior of the chain, as indicated by the differences between our theoretical results for the two different side-chain representations. From the comparison of these results with the experimental data, we conclude that the alignments of side chains are greater in tetrahydrofuran than in benzene. This conclusion is also consistent with the fitting of the data obtained in the latter solvent to a wormlike chain of lower cross section in the range of longer chains, $n > 100$.

The results in tetrahydrofuran for very short chains exhibit a deviation downward with respect to the rigid side chain representation, which can be explained by the more important role played by the terminal branches in these chains. The terminal side chains should be more flexible since they are free of some of the intramolecular interactions. The benzene solutions, however, give deviations upward with respect to the flexible side chain representation in this region. This may be explained by assuming a complicated type of polymer–solvent ordering or by some noticeable degree of alignment for the whole range of molecular weights in this solvent that could be more accurately described by a side-chain representation intermediate between those considered through our calculations.

We finally remark that our discrete model, though only approximate, is able to give a reasonably good description for the low molecular weight hydrodynamic behavior of these complicated comblike structures, which cannot be described adequately by simpler parametric chain models. Nevertheless, the incorporation of further details into the model, obtained through rigorous conformational studies together with the consideration of semistiff side-chain representations and the introduction of the backbone excluded volume, may result in a noticeable improvement of the model performance.

Registry No. Poly[*N*-(*n*-octadecyl)maleimide], 26714-93-2.

References and Notes

(1) Barrales-Rienda, J. M.; Romero Galicia, C.; Freire, J. J.; Horta, A. *Macromolecules*, companion paper in this issue (Part 2).
(2) Sutter, W.; Burchard, W. *Makromol. Chem.* **1978**, *179*, 1961.
(3) Zimm, B. H. *Makromol. Chem., Suppl.* **1975**, *1*, 441.
(4) Zimm, B. H. *Macromolecules* **1980**, *13*, 592.
(5) Yamakawa, H. "Modern Theory of Polymer Solutions"; Harper and Row: New York, 1971.
(6) Garcia de la Torre, J.; Bloomfield, V. A. *Biopolymers* **1978**, *17*, 1605.
(7) Fixman, M.; Kovac, J. *J. Chem. Phys.* **1974**, *61*, 4939.
(8) Ptitsyn, O. B.; Eizner, Yu. E. *Zh. Tekhn. Fiz.* **1959**, *29*, 1117.
(9) Flory, P. J. "Statistical Mechanics of Chain Molecules"; Wiley: New York, 1969.
(10) Sheremeteva, T. V., Larina, G. N.; Tsvetkov, V. N.; Shtennikova, I. N.; *J. Polym. Sci. Part C* **1968**, *22*, 185.
(11) Mason, R. *Acta Crystallogr.* **1961**, *14*, 720.
(12) Freire, J. J.; Horta, A. *J. Chem. Phys.* **1976**, *65*, 4049.
(13) Horta, A.; Fixman, M. *J. Am. Chem. Soc.* **1968**, *90*, 3048.
(14) Tsuda, K. *Rheol. Acta* **1970**, *9*, 509.
(15) Garcia de la Torre, J.; López, M. C.; Tirado, M. M.; Freire, J. J., manuscript in preparation.
(16) Yamakawa, H.; Fujii, M. *Macromolecules* **1974**, *7*, 128.
(17) Yamakawa, H.; Yoshizaki, T. *Macromolecules* **1980**, *13*, 633.
(18) Yamakawa, H. *Macromolecules* **1977**, *10*, 692.
(19) Yoshizaki, T.; Yamakawa, H. *J. Chem. Phys.* **1980**, *72*, 57.